ARTICLE INFORMATION

Article title

Experimental and numerical data from comparative analysis of candidate structural models for active camber morphing wings

Authors

Ke Huang, Jiaying Zhang.*

Affiliations

School of Aeronautic Science and Engineering, Beihang University, Beijing 100190, China

Corresponding author's email address and Twitter handle

jiaying.zhang@buaa.edu.cn

Keywords

active camber morphing wing, stepped cantilever plate, modal test data, 3D printing, finite element model.

Abstract

This data article presents modal test data for 30 specimens: 10 uniform and 20 stepped cantilever plates fabricated from FDM‑printed PLA and CNC‑machined aluminum. The dataset includes modal frequencies and mode shapes measured by scanning laser Doppler vibrometry (SLDV) using chirp excitation (3200 FFT lines). Numerical modal data are provided from finite element models (ABAQUS for uniform plates; Nastran for stepped plates) using beam, shell, solid, beam‑beam, beam‑plate coupled, and plate‑plate formulations. Material parameters are obtained from tensile tests on 21 PLA specimens with seven print orientations to characterize anisotropy. The reusable data comprise raw modal spectra, material stress‑strain curves, manufacturing tolerance measurements, FEM input files (inp and bdf), CAD models (stp), and modal animations. This data article supports the companion research article "Comparative modal analysis of beam-plate coupled models for isotropic active camber morphing wings" and provides a standalone benchmark for validating structural models of rigid‑flexible coupled morphing wings.

SPECIFICATIONS TABLE

[Instruction for SPECIFICATIONS TABLE in comment box]

Subject	Engineering & Materials science
Specific subject area	*Structural dynamics, morphing wing structures, finite element modelling*

Type of data	*Tables, Graphs/Figures, Videos (Modal Shape), Excel file (Test data), Inp files (FEM model), BDF flies (FEM model), STP files (3D printing model)*.
Data collection	*All specimens were manufactured using a Bambu X1C FDM 3D printer with Bambu PLA Basic filament (1.75 mm diameter). Slicing was performed with Bambu Studio software, and the corresponding manufacturing accuracy is documented in the data files. Uniaxial tensile tests were carried out on a SUNS UTM4503 testing machine equipped with a Transcell BSS-500 kg load cell (accuracy class 0.03) and a standard extensometer SUNS YSJ50-ZC (output sensitivity 2mV/V). A standard extensometer was used to record deformation, and the loading rate was maintained at 20 mm/min. Linear vibration measurements were conducted using a Polytec PSV-400 scanning vibrometer. Frequency response data were acquired through chirp excitation signals within the relevant frequency range. A rectangular window function was applied, and 3200 FFT lines were used for spectral analysis. Detailed information on the frequency range and resolution is provided in the data files.*
Data source location	*Institution: Beihang University* *City/Town/Region: Beijing* *Country: China.*
Data accessibility	Repository name: *Mendeley Data* Data identification number: *10.17632/8jxw5533py.2* Direct URL to data: *https://data.mendeley.com/datasets/8jxw5533py/2*
Related research article	*K. Huang and J. Zhang. "Comparative modal analysis of beam-plate coupled models for isotropic active camber morphing wings." Aerospace Science and Technology 178 (2026): 112,449. [1]*

VALUE OF THE DATA

- This dataset provides systematic experimental and numerical modal data for both uniform and stepped cantilever plates, where the stepped configuration (thicker rigid section and thinner flexible section) directly represents the stiffness distribution of active camber morphing wings. It covers aspect ratios from 3 to 6 and flexible segment ratios from 25% to 75%, offering a broad and consistent benchmark for validating beam, plate, and beam–plate coupled models.
- Beyond modal frequencies and mode shapes, this dataset uniquely integrates raw experimental modal spectra from scanning laser Doppler vibrometry, detailed material characterization of FDM–printed PLA across seven print orientations (21 tensile specimens), manufacturing tolerance measurements for every specimen, and ready–to–use finite–element model files (ABAQUS for uniform plates, Nastran for stepped plates) along with modal

animations. This multi–level integration supports comprehensive validation workflows, from material input to final modal response.

- Detailed analysis of the inherent anisotropy of FDM 3D-printed PLA specimens is included. The data report the influence of different print orientations on elastic modulus and failure stress, supplying material parameters that can support structural modelling of 3D-printed specimens.
- Finite element modal analyses based on multiple structural theories are provided, together with model files and calculation details. The comparative results highlight the balance between computational accuracy and efficiency.
- The dataset contributes to improving the prediction of natural frequencies and vibration modes in nonuniform stiffness distributed structures, particularly morphing wing structures. It also demonstrates strategies to address challenges such as material anisotropy and manufacturing tolerances, thereby enhancing the reliability and quality of future modal experiments. The dataset may also support aeroelastic design, flutter control, and the validation of digital twin models.

BACKGROUND

Active camber morphing wings consist of a stiff leading edge spar and a compliant trailing edge, creating a nonuniform stiffness distributed structure [2, 3]. Accurate prediction of their natural frequencies and vibration modes is essential for aeroelastic design [4, 5]. However, existing structural models, including beam model, plate/shell model, and their variants, have not been systematically validated against modal data for configurations that capture this nonuniform stiffness distribution [5, 6]. Stepped cantilever plates, which feature a thicker rigid section and a thinner flexible section, serve as representative benchmarks. Yet open experimental and numerical datasets covering a range of aspect ratios (*AR*) and flexible segment ratios (f_{ef}) are lacking.

This dataset addresses this gap by providing modal test data for uniform and stepped cantilever plates fabricated from FDM printed PLA and CNC machined aluminum, with *AR* from 3 to 6 and f_{ef} from 25% to 75%. In addition, the dataset systematically characterizes the anisotropic behaviour of FDM–printed PLA[7] through tensile tests on 21 specimens with seven different print orientations. The objective of this data article is to provide a comprehensive, openly accessible experimental and numerical dataset (including raw modal data, material characterization, FEM files, and CAD models) for uniform and stepped cantilever plates, to support validation of structural models for camber morphing wings.

DATA DESCRIPTION

Unlike the companion research article , which presents theoretical model comparisons and selection guidelines, this data article focuses solely on describing and providing access to the experimental and numerical dataset [1]. The dataset [8] contains modal test specimens with a fixed width of 50 mm, where the dimensions are determined by two parameters: the aspect ratio (AR) and the flexible segment ratio (f_{ef}). The specimens are illustrated in Fig. 1(a). Based on geometric configuration, the dataset includes two categories of specimens: uniform cantilever plates and stepped cantilever plates.

Active camber morphing wings consist of a stiff leading-edge spar and a compliant trailing edge, creating a nonuniform stiffness distribution structure (see companion article [1], Fig. 2). In such wings, the stiffness difference between the two parts can reach two orders of magnitude. To mimic this stiffness distribution in a simple laboratory specimen, the present dataset introduces the stepped cantilever plate: a rectangular plate with a thicker rigid section (t_R =4 mm) and a thinner flexible section (t_F =1 mm). The thickness change occurs at a distinct step, and the plate is clamped at the rigid end. This stepped configuration directly represents the mechanical idealisation used in the companion study [1], where the rigid part is modelled as a beam (high aspect ratio, prone to bending and torsion) and the flexible part as a plate (low aspect ratio, capturing chordwise bending).

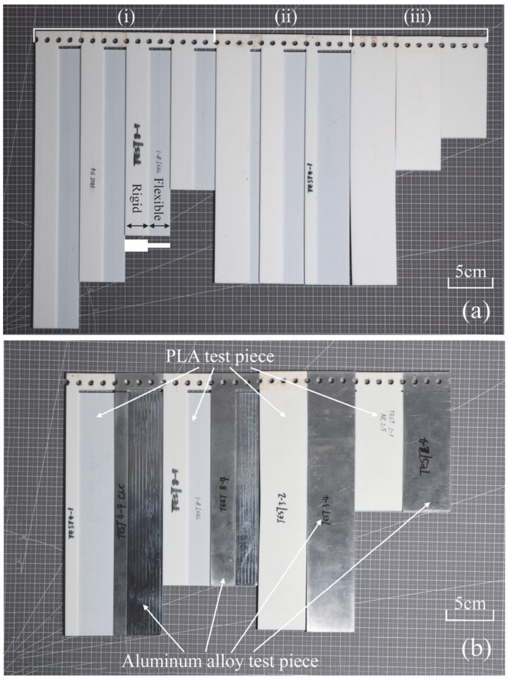

Figure 1. Experimental specimens. (a) 3D printed PLA test pieces. Stepped cantilever plates with (i) different ARs and (ii) different flexible segment ratios. (iii) Uniform cantilever plates with different ARs. (b) aluminum alloy test pieces (adapted from [1]).

For the uniform cantilever plate specimens, the thickness is t = 4 mm. The stepped cantilever plates consist of a rigid section and a flexible section, with thicknesses t_R = 4 mm and t_F = 1 mm, respectively. Two types of manufacturing processes and materials were used: PLA specimens manufactured by FDM 3D printing and aluminum alloy specimens manufactured by CNC machining, as compared in Fig. 1(b).

Table 1. Specimen indices and corresponding geometric dimensions, materials, print orientations, and replicates.

Test No.	Category	AR	f_{ef} (%)	Material	*Build orientation*	*Replicates*
1	Uniform Cantilever Plate	1.8		PLA	flat, on-edge	3
2		2.5		PLA / Al (CNC)	flat, on-edge	3 / 1
3		5.0		PLA / Al (CNC)	flat, on-edge / –	3 / 1
4	Stepped Cantilever Plate	5.0	25	PLA	flat, on-edge	3
5		5.0	50	PLA	flat, on-edge	3
6		5.0	75	PLA / Al (CNC)	flat, on-edge / –	3 / 1
7		6.0	50	PLA	flat, on-edge	3
8		4.0	50	PLA	flat, on-edge	3
9		3.0	50	PLA / Al (CNC)	flat, on-edge / –	3 / 1

The dataset consists of Excel files, finite element model files, and 3D models of the specimens. Specifically, it includes 7 Excel data files and four folders. The four folders contain:

- ABAQUS inp files for finite element models,
- Nastran bdf files for finite element models,
- 3D CAD models (stp format) of all specimens,
- Modal animation files corresponding to different vibration modes of the specimens.

All specimens were labelled in the format Test X–Y, where X denotes the specimen group with different geometric dimensions, and Y specifies the manufacturing process or print orientation. Specifically, Y = 1–3 corresponds to three repeated FDM 3D-printed specimens with different print orientations, while Y = 4 refers to the CNC-machined aluminum alloy specimen. In the folder named "FDM Stp Files", the 3D models are organized using the format Test X, corresponding to the different specimen geometries. The mapping of index X to specimen geometry is summarized in Table 1.

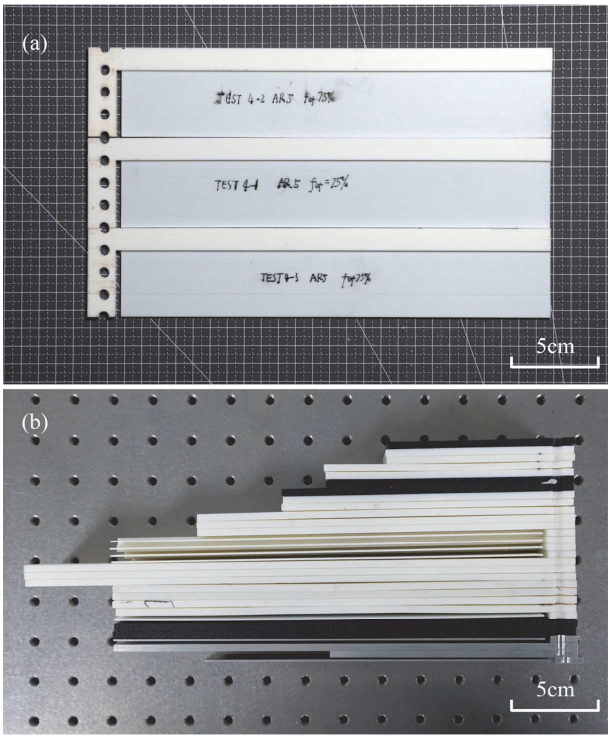

Figure 2. (a) Repeated specimens of Test–6 showing two print orientations. (b) Complete set of experimental specimens (uniform and stepped plates; PLA and aluminum).

Each specimen used in this study was manufactured in triplicate using FDM 3D printing, with two different print orientations adopted to mitigate printing-induced material anisotropy. Figure 2(a) shows the repeated specimens for Test-6, while Figure 2(b) illustrates the all specimens employed in the experiments. For all modes, the frequencies were nondimensionalized, and mean values and standard deviations were calculated. This procedure minimizes the influence of measurement and material uncertainties, ensuring that the observed deviations mainly reflect differences between numerical or theoretical models.

To evaluate the manufacturing accuracy of the Bambu X1C FDM 3D printer, 25 calibration cubes with an edge length of 20 mm were fabricated. The dimensions along all three axes, together with their means and standard deviations, are provided in the file "2-1 Tolerance inspection of FDM 3D printer.xlsx". The corresponding 3D model is available in the folder "FDM Stp Files" as "XYZ Calibration cube.STEP". The actual dimensions of all test specimens are given in "2-2 Specimen tolerance.xlsx", where model size refers to the nominal design values, actual size 1–5 denote five independent measurements, and the table also includes mean values, tolerances, and dimensional errors. The data file specifies the manufacturing method for each specimen.

To analyse anisotropy induced by the FDM process, specimens were manufactured in seven build orientations, as shown in Fig. 3. Four principal orientations were considered: along the X-axis, Y-axis, 45° to the −Y-axis, and Z-axis (upright). For the X, Y, and 45° orientations, specimens were produced both flat (thickness perpendicular to the print bed) and on-edge (thickness parallel to the print bed). Three replicates were fabricated for each type to assess repeatability. All material specimens follow the ASTM D638-22 Type I geometry, with the 3D model provided in "FDM Stp Files" as "ASTM D638-22_TYPE1_Test Specimen.STEP" [9].

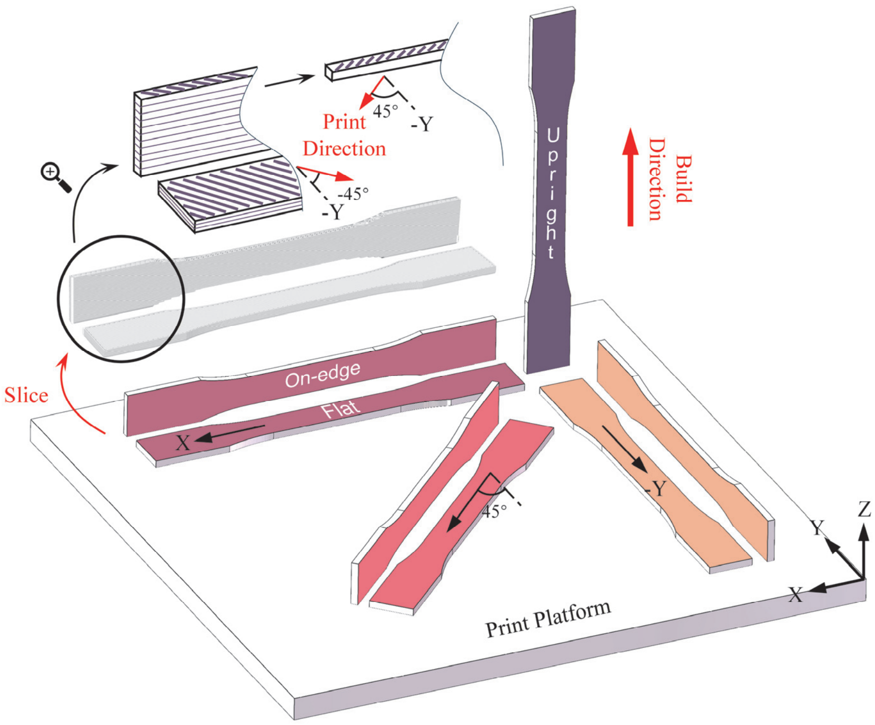

Figure 3. Process parameters and layer patterns for standardized test specimens (adapted from [1]).

Specimens were labelled using the format (A)–(B)–(C), where A denotes the build orientation, B indicates position (O: on-edge, F: flat, U: upright), and C is the replicate number. The raw uniaxial tensile data are contained in "3-2 Original data of material tests.xlsx", including force (N), crosshead displacement (mm), extensometer deformation (mm), stress (MPa), and strain. The processed mechanical properties, including elastic modulus (MPa) and ultimate strength (MPa), are summarized in "3-1 Material property.xlsx", which also provides mean values and standard deviations across different build orientations and manufacturing conditions.

3.1 Uniform cantilever plate

For the uniform cantilever plate specimens, aspect ratios of 1.8, 2.5, and 5.0 were tested. Additional CNC-machined aluminum specimens with AR = 2.5 and AR = 5.0 were prepared as linear-elastic references to evaluate the influence of 3D printing on material properties. With three repeated specimens per geometry, this set includes nine 3D-printed and two CNC aluminum specimens. Numerical models were developed in ABAQUS 2024 to calculate the first 20 natural frequencies. In all ABAQUS models, the clamped boundary condition was applied by fixing all six degrees of freedom (UX, UY, UZ, RX, RY, RZ) at the root.

All models are available in the folder named "ABAQUS inp Files", where files are labelled as AR(X)_(Y), with X denoting the aspect ratio and Y the structural model. For solid elements, the suffix "SOLID" followed by the mesh size(mm) is specified, while all other element sizes were set to 0.5 mm. An element size of 0.5 mm was adopted to ensure mesh independence. The following element types were used in ABAQUS: B33 and B32 for beam models (Euler and Timoshenko beams, respectively), S8R5 for thin shells, S8R for thick shells, and C3D8R for solid elements.

Frequencies are compared using the nondimensional form $\Omega_{\mathrm{u}} = \omega L^2/\sqrt{\rho t/D}$, where ω is the resonance angular frequency, ρ the material density, and $D = Et^3/[12(1-\nu^2)]$ the bending stiffness with E and ν the Young's modulus and Poisson's ratio.

Experimentally measured mode shapes are provided as animations in the subfolder "Uniform cantilever plate" under "Modal Animation Video Files". All modal animation videos are named using the format AR(X)_(Y)(Z), where X denotes the aspect ratio, Y indicates the mode number (order), and Z specifies the mode type: B for spanwise bending, T for torsion, and FB for chordwise bending.

3.2 Stepped cantilever plate

For the stepped cantilever plate specimens, six groups were tested: AR = 5 with flexible segment ratios of 25%, 50%, and 75%, and AR = 3, 4, and 6 with f_{ef} = 50%. Additional CNC aluminum specimens were prepared for AR = 5, f_{ef} = 75% and AR = 4, f_{ef} = 50%. Each group contains three repeated specimens, yielding 18 3D-printed and two CNC aluminum specimens in total. Numerical models were developed in Nastran to calculate the first 20 natural frequencies, using a uniform element size of 0.5 mm. An element size of 0.5 mm was adopted to ensure mesh independence. The Nastran models used CBEAM elements for beam representations and CQUAD4 elements for plate representations. Rigid connections between the two parts were simulated using RBAR elements, ensuring displacement compatibility at the connection nodes. Candidate structural models include the plate-plate (PP), beam-plate (BP) coupled, and beam-beam (BB) models, as illustrated in Fig. 4. The single point constraints (SPC) labelled '123456' indicate that all six degrees of freedom (UX, UY, UZ, RX, RY, RZ) at the constrained nodes are fixed to represent the clamped end. An element size of 0.5 mm was adopted to ensure mesh independence.

All models are provided in the folder named "Nastran bdf Files", with filenames in the format AR(X)fef(Y)(Z)Model, where X denotes aspect ratio, Y the flexible segment ratio, and Z the structural model type. Frequencies are compared using the nondimensional form $\Omega_s = \omega L^2/\sqrt{\rho t_R/D_R}$, where $D_R = Et_R^3/[12(1-\nu^2)]$.

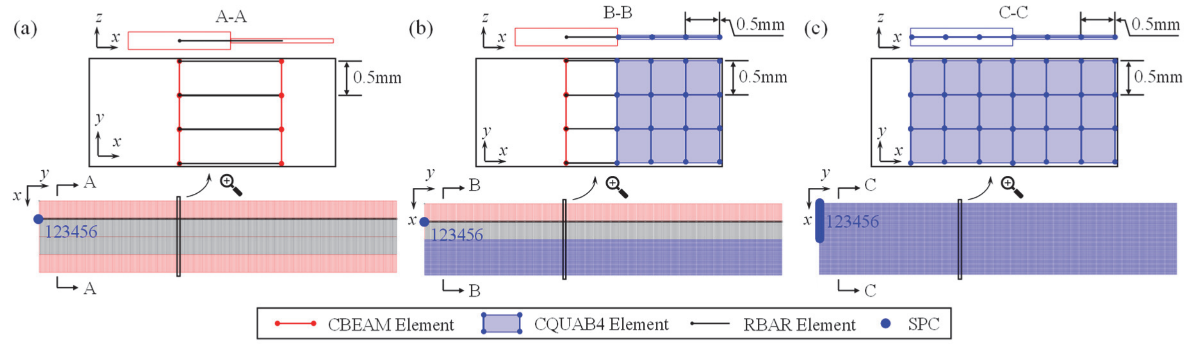

Figure 4. Finite element models. (a) Beam-Beam model. (b) Beam-Plate coupled model. (c) Plate-Plate model. Side views and local zoom-ins are shown for illustrative purposes, with mesh sizes intentionally exaggerated for clarity (adapted from [1]).

Experimentally measured mode shapes are provided as animations in the subfolder "Stepped cantilever plate" under "Modal Animation Video Files". All modal animation videos are named using the format AR(X)fef(K)_(Y)(Z), where X denotes the aspect ratio, K denotes flexible segment ratios, Y indicates the mode number (order), and Z specifies the mode type: B for spanwise bending, T for torsion, and FB for chordwise bending.

Table 2. Definitions of symbols and abbreviations used in this article and dataset.

Symbol	Description	Abbreviation	Description
AR	Aspect ratio	BB	Beam−beam model
f_{ef}	Flexible segment ratio	BP	Beam−plate coupled model
Ω_u	Nondimensional angular frequency for uniform cantilever plate	PP	Plate−plate model
Ω_s	Nondimensional angular frequency for stepped cantilever plate	Dim	Nondimensional frequency normalized by the first bending frequency
t_R	Thickness of rigid section	B	Bending mode
t_F	Thickness of flexible section	T	Torsion mode
D_R	Bending stiffness of rigid section	FB	Chordwise bending mode

All experimental and numerical modal frequencies, together with their nondimensional forms, are provided in "1-1 Modal test experiment and numerical results.xlsx". Mode numbers denote the order, while B, T, and FB correspond to spanwise bending, torsion, and chordwise bending modes, respectively. Dim represents nondimensional frequencies normalized by the first bending frequency, and Dim_u represents frequencies nondimensionalized by material and geometric parameters. The dataset includes:

- Experimental and numerical modal frequencies (Hz) and nondimensional frequencies for all specimens.
- Mean, standard deviation, and coefficient of variation (Cv, %) of Dim_u obtained from repeated specimens.
- Frequencies, nondimensional frequencies, and errors calculated from all numerical models.
- Comparison of nondimensional frequencies between CNC specimens and PLA 3D-printed specimens.
- Frequency sweep ranges, scan point densities, and scan duration time (s) for each point.

The original scan spectra from modal tests are available in "1-2 Original data of modal tests.xlsx", including vibration velocity frequency (Hz) and magnitude (m/s).

The symbols and abbreviations used in this article are defined in Table 2.

Computation efficiency and accuracy of all numerical models are summarized in "4-1 FEM detail.xlsx". This file provides details of the computational platform, element types, numbers of elements, nodes, and degrees of freedom, computation time (s), and maximum errors (%) for bending and torsional modes.

To facilitate navigation and reuse of the dataset, a Data Map is provided in Table 3. It links each data file or folder to its content, and the specimen groups.

Table 3. Definitions of symbols and abbreviations used in this article and dataset.

File/Folder	Description	Specimen Group
1-1 Modal Test Experiment and Numerical Results.xlsx	Experimental & numerical modal frequencies, dimensionless ratios, relative errors	All (uniform + stepped)
1-2 Original data of modal tests.xlsx	Raw FRF spectra (frequency, velocity magnitude, phase)	All
2-1 Tolerance inspection of FDM 3D printer.xlsx	Dimensional deviations of 25 calibration cubes	Calibration cubes
2-2 Specimen tolerance.xlsx	Actual measured dimensions of every specimen	All
3-1 Material property.xlsx	Mean ± SD of Young's modulus & ultimate strength for 7 orientations	Tensile specimens
3-2 Original data of material tests.xlsx	Raw stress-strain curves for 21 specimens	Tensile specimens
4-1 FEM Detail.xlsx	Element types, node/element counts, DOFs, computation time, errors	All
ABAQUS inp Files	FEM input files for uniform cantilever plates (Abaqus/Standard 2024)	Uniform cantilever plates
Nastran bdf Files	FEM input files for stepped cantilever plates (Nastran 2020)	Stepped cantilever plates
FDM Stp Files	3D CAD models (STEP format) of all specimens	All
Modal Animation Video Files	Animated mode shapes for uniform and stepped cantilever plates	All

EXPERIMENTAL DESIGN, MATERIALS AND METHODS

4.1 Test Specimens Preparation

All specimens were prepared and tested at the Advanced Aerostructure Dynamics Research (Astar)-Lab, Beihang University. PLA specimens were fabricated using a Bambu X1C FDM 3D printer with Bambu PLA Basic filament (1.75 mm diameter). Slicing was performed in Bambu Studio. The layer height was set to 0.08 mm and the raster width to 0.42 mm, with 100% infill in a rectilinear pattern. The nozzle diameter was 0.4 mm, the extrusion temperature 220 °C, and the infill speed 350 mm/s.

The stepped cantilever plate is fabricated as a monolithic piece with a sudden thickness change at a location determined by the flexible segment ratio f_{ef} (25%, 50%, or 75% of the chord). No adhesive or mechanical joint is used between the two sections, ensuring a clean stiffness transition.

4.2 Manufacturing variability and boundary condition repeatability

To account for manufacturing variability, three replicate specimens were fabricated for each geometric configuration and print orientation. Two distinct build orientations (flat and on-edge) were used for the X-axis, Y-axis, and 45° specimens, while upright orientation was used for Z-axis specimens. The dimensional accuracy of the FDM printer was assessed by printing 25 calibration cubes (20 mm edge length) and measuring their dimensions along three axes. The measured deviations (mean ± standard deviation) were 0.016±0.028 mm (X-axis), 0.056±0.029 mm (Y-axis), and 0.020±0.015 mm (Z-axis).

Additionally, five key dimensions of every test specimen were manually measured using a micrometer (resolution 0.001 mm) to correct the nominal design values in subsequent finite-element analyses. The combined effect of manufacturing variability is reflected in the standard deviations of modal frequencies reported for each specimen group.

To ensure repeatability of the clamped boundary condition, the specimen was mounted in a custom-designed clamping fixture with the clamping bolts. For each new specimen, the clamping fixture was completely loosened, the specimen was repositioned to ensure a consistent embedment length (10 mm from the root), and then the bolts were re-tightened. This procedure was repeated for every specimen, including all three replicates. The consistency of experimental results across multiple specimens (see standard deviations in file '1-1 Modal Test Experiment and Numerical Results.xlxs') indirectly validates the repeatability of the clamping procedure.

4.3 Material Test

3D-printed material specimens were tested under uniaxial tension using a SUNS UTM4503 universal testing machine, equipped with a Transcell BSS-500 kg load cell (accuracy class 0.03) and a standard extensometer SUNS YSJ50-ZC (output sensitivity 2mV/V). The loading speed was 20 mm/min, and the standard extensometer recorded the deformation. Material testing followed ASTM D638 standards.

Figure 5(a) shows the experimental setup, and Fig. 5(b) presents the fabricated specimens. Figures 5(c) and 5(d) illustrate representative stress–strain curves for different print orientations, along with the mean responses and error bands for all specimens.

Material property uncertainty was systematically characterized through tensile tests on 21 specimens manufactured with seven different print orientations (X-axis flat/on-edge, Y-axis flat/on-edge, 45° flat/on-edge, and Z-axis upright), with three replicates per orientation. The raw stress-strain data for all 21 specimens are provided in file '3-2 Original data of material tests.xlsx'. The mean Young's modulus and ultimate strength for each orientation, along with their standard deviations, are summarized in file '3-1 Material property.xlsx'. The overall Young's modulus of the 3D-printed PLA was 2.113 ± 0.105 GPa (coefficient of variation $\approx$ 5.0%), representing the combined uncertainty from filament batch variability, printer calibration, and orientation-dependent anisotropy.

Table 4. Summary of tensile test results for FDM−printed PLA specimens.

Print orientation	Maximum strength (MPa)	Elastic modulus (MPa)
X-axis flat	36.05 ± 1.40	2047.3 ± 94.9
X-axis on-edge	41.85 ± 0.34	2267.4 ± 83.8
Y-axis flat	34.47 ± 3.96	1958.4 ± 111.6
Y-axis on-edge	38.19 ± 3.65	2206.5 ± 45.7
45° flat	38.33 ± 3.45	2043.6 ± 93.5
45° on-edge	35.28 ± 6.73	2106.6 ± 158.9
Z-axis upright	27.63 ± 1.63	2122.4 ± 53.4
Overall (all orientations)	36.31 ± 6.02	2079.9 ± 146.2

Table 4 summarizes the tensile test results for all 21 FDM−printed PLA specimens. The specimens were fabricated with seven different print orientations: X−axis flat, X−axis on−edge, Y−axis flat, Y−axis on−

edge, 45° flat, 45° on−edge, and Z−axis upright, with three replicates per orientation. The table reports the mean and standard deviation of maximum strength (MPa) and elastic modulus (MPa) for each orientation, as well as the overall mean and standard deviation across all 21 specimens.

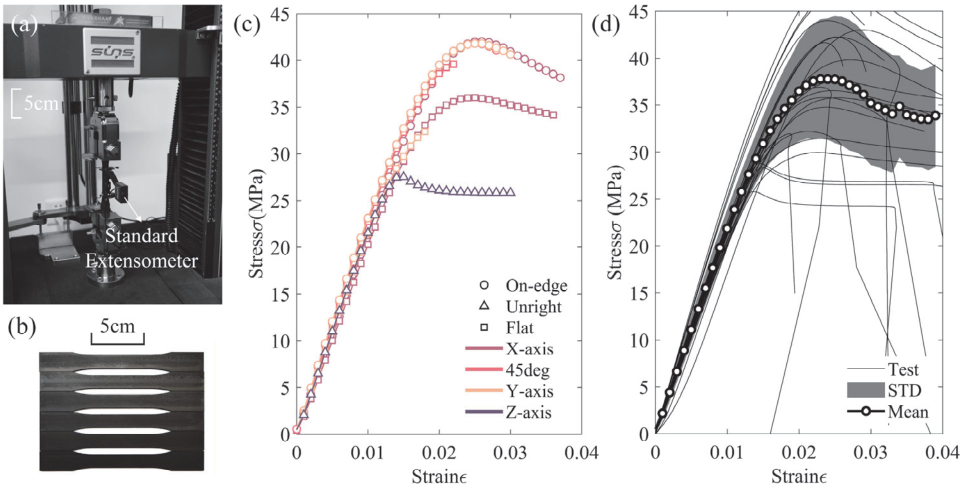

Figure 5. Mechanical properties testing: (a) Experimental setup. (b) Test specimens. (c) Representative stress–strain curves for different printing orientations. (d) Mean stress–strain curves of all specimens with error bands (adapted from [1]).

Mass measurements were performed using a Kubei electronic balance with a capacity of 0.2–5000 g and a resolution of 0.01 g. To further evaluate material density, a standard calibration cube with a 20 mm edge was printed using the same FDM process (Fig. 6(a)). The mass of five filament samples (50 cm length, 1.75 mm diameter) was measured, yielding an average density of 1184 kg/m³ with a standard deviation of 4.8 kg/m³ (Fig. 6(b)). The cube volume was 7505.83 mm³, giving a calculated mass of 8.89 g based on the measured density. Measurements of 25 calibration cubes produced an average mass of 8.57 g with an uncertainty of 0.01 g. Although the nominal infill ratio was set to 100%, the actual infill ratio was approximately 97.16%.

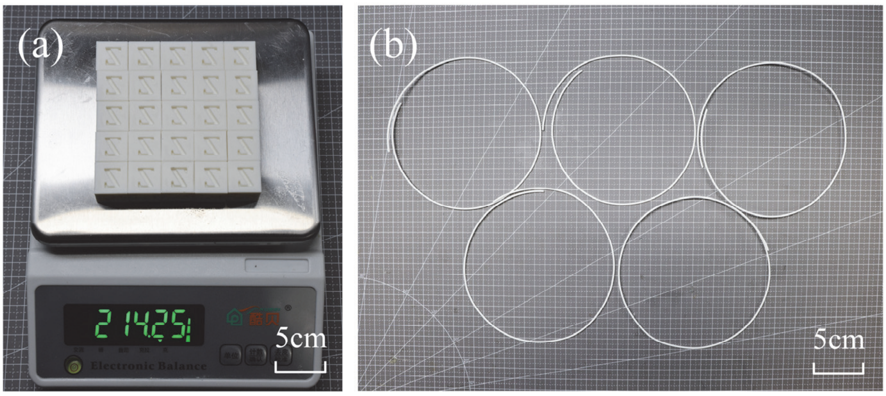

Figure 6. Mechanical properties testing: (a) Standard calibration cube. (b) Filament samples.

4.4 Modal Experiment Setup

The experimental setup is shown in Fig. 7(a)–(c). Linear vibration measurements were performed using a Polytec Scanning Vibrometer (PSV)-400, equipped with a PSV-I-400 MR laser head and an NI 4451 signal generation and data acquisition module.

The Polytec PSV–400 scanning vibrometer has a specified velocity resolution of 10 µm/s/V (for the PSV–I–400 MR head). To assess the repeatability of the non-contact measurement system, three consecutive modal tests were performed on the same specimen without changing any setup parameters, using two CNC-machined aluminum alloy specimens: Test4-4 (uniform cantilever plate, AR=5, CNC-machined aluminum) and Test8-4 (stepped cantilever plate, AR=4, fef=50%, CNC-machined aluminum). The three repeated tests were conducted with complete remounting of the specimen each time. The natural frequencies obtained from the three repeats showed no significant differences, demonstrating excellent stability and repeatability of the PSV-400 measurement system. The raw frequency data from these repeatability tests are included in the file '1-1 Modal Test Experiment and Numerical Results.xlsx'. For the 3D-printed specimens, the standard deviations reported across three independent replicate specimens (manufactured separately) inherently include additional variability from manufacturing and material, which are larger than the pure measurement repeatability.

Modal frequencies were extracted from the measured frequency response functions (FRFs) using the commercial software PSV 9.0 (Polytec GmbH). The specific peak-picking algorithm is proprietary and not disclosed by the manufacturer. The operational procedure followed standard practices: for each scan point, the point FRF was computed from the chirp excitation signal (rectangular window, 3200 FFT lines). Natural frequencies were identified as the peaks in the averaged FRF (averaged over all scan points). Mode shapes (bending, torsion, chordwise bending) were classified by visualizing the animated deformation from the scanning data and by comparing the phase information across scan points.

Frequency sweeps were performed with periodic chirp signals covering the relevant structural response range. A rectangular window function was applied, and 3200 FFT lines were used for signal analysis.

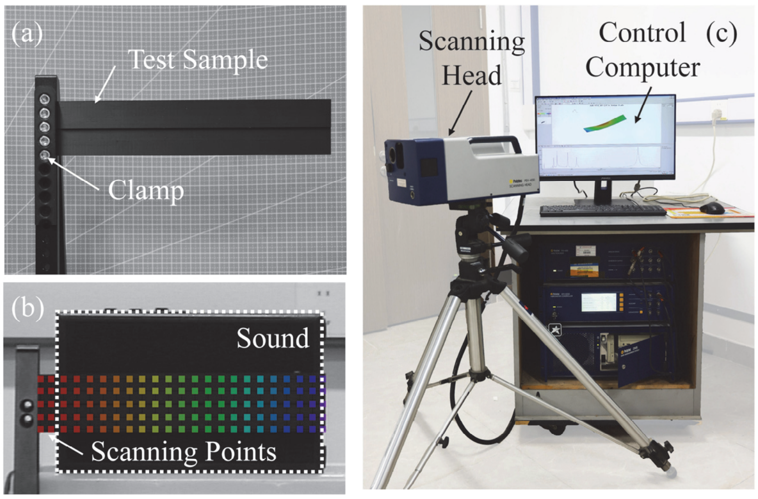

Figure 7. Non-contact modal testing setup. (a) Specimen mounting and support configuration. (b) Excitation source and scanning area. (c) Polytec PSV-400 scanning vibrometer setup (adapted from [1]).

The excitation source was a loudspeaker generating periodic chirp signals. Scan point densities varied with specimen geometry: for uniform plates of AR=1.8,2.5,5.0, the spanwise and chordwise point counts were (7×3), (9×3), (9×5) respectively; for stepped plates, typical densities were (9×5) to (11×3) (see file '1-1' for each specimen). Frequency resolution was 0.25 Hz for the 0–800 Hz range, 0.39 Hz for the 0–1250 Hz range, and 0.78 Hz for the 0–2500 Hz range. Mode shapes were classified as spanwise bending (B), torsion (T), or chordwise bending (FB) by visualizing the animated deformation from the scanning data and by comparing the phase information across scan points.

LIMITATIONS

This study demonstrates the beam–plate coupled model offers advantages in both computational accuracy and efficiency. However, several limitations of the current dataset should be noted.

- This dataset is best suited as a baseline for validating simplified structural models (beam, plate, and beam-plate coupled) under linear-elastic, isotropic, small-amplitude vibration conditions. For applications involving large deformations, hyperelastic or viscoelastic polymers, anisotropic composites, or preload-dependent configurations, users should treat the dataset as a reference for comparison rather than a direct validation target. The provided raw data (modal spectra, material stress-strain curves, tolerance measurements) may be used to build upon this baseline by incorporating appropriate nonlinear material laws, contact conditions, or geometric modifications. Future users are encouraged to extend the dataset accordingly and to validate their extended models against the presented baseline results.
- Geometric imperfections are not incorporated into the nominal numerical models; actual measured dimensions are provided separately.
- The current models are relatively simple and do not fully represent the complex structural features of morphing wings. It remains to be evaluated whether the rigid leading edge can be accurately represented by a statically condensed beam and the flexible trailing edge by an equivalent plate with varying inertia and stiffness.
- The modelling of connection stiffness between leading and trailing edges, as well as the handling of complex, discontinuous stiffness distributions and structural anisotropy, requires further investigation.

ETHICS STATEMENT

The authors have read the ethical requirements for publication in Data in Brief and confirm that the current work does not involve human subjects, animal experiments, or any data collected from social media platforms.

CRediT AUTHOR STATEMENT

Ke Huang: Writing – original draft, Investigation, Data curation. **Jiaying Zhang:** Writing – review & editing, Supervision, Conceptualization.

ACKNOWLEDGEMENTS

This project has received funding from National Natural Science Foundation of China (Grant No. 92271104, 12102017) and Beijing Natural Science Foundation (Grant No. 1232014).

DECLARATION OF COMPETING INTERESTS

- The authors declare that they have no known competing financial interests or personal relationships that could have appeared to influence the work reported in this paper.

REFERENCES

[1] K. Huang, J. Zhang, Comparative modal analysis of beam-plate coupled models for isotropic active camber morphing wings, Aerospace Science and Technology, 178 (2026) 112449.

[2] J. Zhang, A.D. Shaw, C. Wang, H. Gu, M. Amoozgar, M.I. Friswell, B.K.S. Woods, Aeroelastic model and analysis of an active camber morphing wing, Aerospace Science and Technology, 111 (2021) 106534.

[3] M.N. Mowla, T. Durhasan, D. Asadi, Z. Kesilmiş, J. Rashid Jafari, Aerodynamic coefficient prediction of bio-inspired camber morphing wings with flexible surfaces using an explainable transformer, Aerospace Science and Technology, 170 (2026) 111557.

[4] M.N. Mowla, D. Asadi, T. Durhasan, J.R. Jafari, M. Amoozgar, Recent advancements in morphing applications: Architecture, artificial intelligence integration, challenges, and future trends-a comprehensive survey, Aerospace Science and Technology, 161 (2025).

[5] Y. Dai, J. Li, Y. Hu, J. Zhang, Y. Zhang, Z. Xi, Y. Zheng, M.I. Friswell, Progress in aerodynamics and aeroelasticity of morphing aircraft, Progress in Aerospace Sciences, 163 (2026) 101206.

[6] S. Yu, X. Zhou, R. Huang, Time-Varying Aeroelastic Modeling and Analysis for a Morphing Wing, AIAA Journal, 62 (2024) 3825-3840.

[7] M. Moradi, A. Aminzadeh, D. Rahmatabadi, A. Hakimi, Experimental investigation on mechanical characterization of 3D printed PLA produced by fused deposition modeling (FDM), Materials Research Express, 8 (2021) 035304.

[8] K. Huang, J. Zhang, Experimental and numerical data from comparative analysis of candidate structural models for active camber morphing wings, Mendeley Data, 2026. doi: 10.17632/8jxw5533py.2

[9] M.R. Khosravani, P. Frohn-Sörensen, A. Schwarzkopf, B. Engel, T. Reinicke, Brittle fracture of notched components fabricated by stereolithography, Journal of Materials Research and Technology, 33 (2024) 8071-8078.